



19th International Conference on Knowledge Based and Intelligent Information and Engineering Systems

Automatic Classification of Facial Morphology for Medical Applications

Hawraa Abbas^{a,c*}, Yulia Hicks^a, David Marshall^b

^aCardiff School of Engineering, Queens Buildings, CF24 3AA, Cardiff, UK.

^bCardiff School of Computer Science and Informatics, Queens Buildings, CF24 3AA, Cardiff, UK.

^cKarbala School of Engineering, Karbala, Iraq.

Abstract

Facial morphology measurement and classification play important role in the face anthropometry of many medical applications. This usually involves the investigation of medical abnormalities where specific facial features are studied by taking a number of measurements of the facial area under investigation. The measurements are often obtained from the three-dimensional (3D) scans of the faces; however, the measurements are often made manually, which is tedious and time consuming process. Moreover, in gene related studies thousands of measurements may be necessary in order to find statistically significant relationships between facial features and genes. Normative studies, from which typical populous models can be built, also require many measurements. Thus an automatic method to extract morphological measurements and interpret them is desirable. In this article, an automatic method for classification of facial morphology on the basis of a number of geometric measurements obtained automatically from 3D facial scans is presented. Among different facial features the philtrum, which is the vertical groove extending from the nose to the upper lip and the lip area, plays an important role in defining the interaction between the genes and craniofacial anomalies such as, for example, cleft lip and palate. In this paper, geometric features are analysed for their suitability to classify philtrum into three classes previously proposed by medical experts. Moreover, further analysis is conducted to assess the best number of classes to model the underlying data distribution from the point of view of classification accuracy. The obtained classification results are compared with the ground truth manual labelling of 3D face meshes provided by a medical expert. The dataset used for this research is taken from ALSPAC dataset and consists of 1000 3D face meshes. The proposed method achieves classification accuracy of 97% for this data set using the Mean, Minimum and Maximum curvature features in combination.

© 2015 The Authors. Published by Elsevier B.V. This is an open access article under the CC BY-NC-ND license

(<http://creativecommons.org/licenses/by-nc-nd/4.0/>).

Peer-review under responsibility of KES International

* Corresponding author. Tel.: +447825885274;
E-mail address: hawrrahassan@yahoo.com

Keywords: 3D face morphology; curvature measurement; ALSPAC dataset.

1. Introduction

A large number of studies related to human face geometry have focused on facial morphology, which provides clinical information on the present or future health conditions of people. Nowadays, 3D face geometry is captured using 3D scanners, either laser or optics-based [1]. In either case, a 3D mesh representing the face geometry is obtained as a result of this process and any consequent face measurements are obtained from the 3D mesh.

The philtrum and its surrounding area form an important part of the human face (Fig. 1). Philtrum is important in diverse applications such as face expression recognition, post-operative patient treatment, and studies of genetic anomalies in facial morphology. There is a number of previous studies in face anthropometry, focused on measuring different parts of the 3D face meshes and classifying them according to their shapes, which in turn have essential role in medical applications such as assessment in cleft lip and nose surgery or finding classification scales which may be utilized to categorise ethnic groups, and to determine genotype/phenotype associations. For example, Mori et al. [2] examined a small data set of 109 samples of five to six years old Japanese children to create standard facial model of normal Japanese children for the lip and nose shape. He calculated manually the distance between labial fissure and Cupid's bow and the width of philtrum part and the nose, which were used to create the model. To classify the lip and mouth parts [3, 4], the main characteristics of the lips and mouth, such as the upper lip and lower lip shapes and the philtrum shape have been reported [3]. Later, Wilson produced a certain measurement of lip vermilion and Cupid's bow. She described different morphological features of the vermilion of the lips and all associated lip traits [4]. However, the measurements of facial morphology are usually performed manually – This is a laborious and monotonous process.

Consequently, the goal of our research is to develop a method for automatic classification of facial features for medical applications. In this preliminary study, we focus on creating such a system for philtrum classification, for which we hope to reproduce the classification results obtained manually by Wilson in [4].

In previous studies, a variety of geometric features and distance measures were used to describe parts of a face, with different types of features showing effectiveness in certain applications. For example, in face recognition applications, Euclidean and geodesic distances, as well as shape and curvedness information were used successfully. On the other hand, in landmark identification applications, the shape index and spin images have been utilised [5]. Among the above features, curvature features are relatively easy to extract and have the property of being invariant to rotation of a given surface, which is important in our application; hence our decision to employ curvature features in this work.

Facial curvature features have been studied and used extensively, with the major applications being in face recognition as a whole [6-8] or as a part [9], face classification [10], and face expression recognition [11]. The mean and Gaussian curvature has been used as a feature describing face regions [6] or for encoding the local shape variation information characterising a particular individual. In the latter case, it was used together with the global geometric features [7]; with the face recognition accuracy was reaching 92% in [6]. Furthermore, the maximum, minimum, Gaussian, and mean curvature were used as features 3D face recognition with a different orientation [8].

In a study on recognition of specific parts of the face, Pflug et al. [9] employed the curvature and semantic analysis of edge patterns to detect the ear in 3D profile face. Pflug's approach was robust against rotation and scaling, with the accuracy of detection reaching nearly 96%.

In 2009, Chen and Biswas [10], focused on the global properties of ranking curvatures for small regions. Both digital Gaussian curvatures and digital mean curvatures of 3D shapes have been used to propose a multi-scale method for 3D object analysis and similar classification. In addition, they showed how the mean curvatures can be used to find local features and extreme points such as nose in 3D facial data [10]. The curvature features are useful but are not necessarily the best features for face expression recognition. Wang et al. [11] applied these features to 3D facial expression recognition. The authors used Support Vector Machin (SVM) classification algorithm on the 100 subjects of the Bosphorus database and a 76.56% recognition rate for six universal facial expressions was achieved [11].

In this study, we have evaluated the curvature features suitability to classify the philtrum face area. We determined the best curvature feature combination to classify the philtrum into the three classes manually predetermined by (an expert) Wilson [4] and investigated the optimal number of classes of philtrum shapes from the point of view of automatic classification. We compared the automatic classification results to the results produced manually by Wilson [4] to assess performance of our system. For the assessment, 1000 3D face meshes were used from ALSPAC dataset with our system achieving 97% classification accuracy in comparison to the ground truth. One of the main challenges in this research was finding the best geometric features to be used in the automatic classification system in order to acquire results close to the manual classification results.

The remainder of this paper is organized as follows. Section 2 describes the curvature concepts and terminology. Next, Section 3 illustrates the methodology and data set that used. Subsequently, Section 4 presents the obtained results. Finally, in Section 5, the findings of this paper are summarized and suggestions for further research are made.

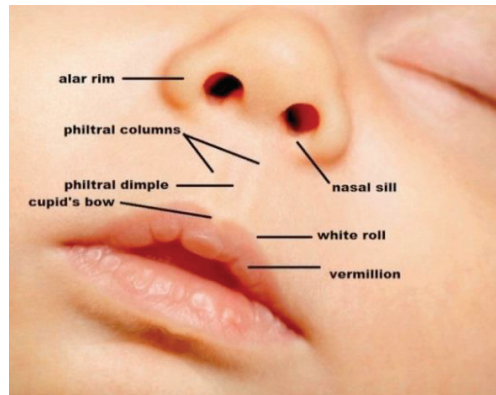


Fig. 1 Philtrum and its surrounding area

2. Curvature concepts and definitions

The curvature of a surface can be defined as how much a curve is bent, or the curvature at any point is how much it locally deviates from the tangent at that point. In a 3D space, the curvature can be defined as

$$k = \frac{\|\ddot{\mathbf{y}} - \dot{\mathbf{y}} * \bar{\mathbf{y}}\|}{\|\dot{\mathbf{y}}\|^2} \tag{1}$$

$$= \frac{\|\dot{\mathbf{y}} * \ddot{\mathbf{y}}\|}{\|\dot{\mathbf{y}}\|^3} \tag{2}$$

where $\mathbf{y}=[x(t)y(t)z(t)]^T$, $t=[uv]^T$, $\dot{\mathbf{y}}$ and $\ddot{\mathbf{y}}$ are the first and second derivatives of the curve, and $\bar{\mathbf{y}}$ is a unit vector represents the curvature target, $\bar{\mathbf{y}} = \dot{\mathbf{y}} / \|\dot{\mathbf{y}}\|$ and the vector $\ddot{\mathbf{y}} - \dot{\mathbf{y}} * \bar{\mathbf{y}}$ is orthogonal to the tangential vector, and when normalized to a unit magnitude it define the normal curve.

There are two kinds of curvatures, the geodesic k_g and the normal curvatures k_n , which are defined by the second derivative vector of the parametric curve on 3D surface. If we represent the 3D surface by u and v parameters

instead of t parameter then the surface will be $\sigma=[x(u,v),y(u,v),z(u,v)]^T$ from which both type of curvature can be calculated as:

$$k_g = \frac{\dot{y}}{\|\dot{y}\|^2} * n * t \tag{3}$$

$$k_n = \frac{\ddot{y}}{\|\dot{y}\|^2} * n \tag{4}$$

where $n = \sigma_v * \sigma_u / \|\sigma_v * \sigma_u\|$, σ_v and σ_u are the derivatives of the surface with respect to u and v , $t = \bar{y}$. from Eq. 4 two unique normal curvature can be found called *minimum* k_1 and *maximum* k_2 normal curvatures, from which two other curvature features can be calculated; the first one is the *mean curvature* $H = (k_1 + k_2) / 2$ and the other one is *Gaussian curvature* $K = k_1 * k_2$ [1].

2.1. 3D Curvature Tensor Estimation

Many methods have been developed to measure or estimate curvature for a smooth or a polyhedral surface[12]. However, the simplest formula to drive curvature measurement is to use the *theory of normal cycles*. This theory provides a unified way to define curvature for both smooth and polyhedral surfaces [13, 14].

The main idea of this theory is that to have a continuous tensor field over the whole surface, a piecewise linear curvature tensor field should be established by estimating the curvature tensor at each vertex and then interpolating these values. Fig 2 shows the principle method to calculate the curvature tensor for each vertex according to the following equation:

$$\mathcal{T}(v) = \frac{1}{|B|} * \sum_{edges} B(e) |e \cap B| \bar{e} e^{-t} \tag{5}$$

where v is a vertex on the mesh, $|B|$ is the surface area around v , $B(e)$ is the signed angle between the normal to the two oriented triangles incident to edge e , $|e \cap B|$ is the length of $e \cap B$ and \bar{e} is a unit vector in the same direction as e [15].

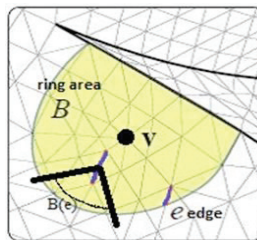


Fig. 2 The integration domain for curvature

Practically, the normal cycle method is fast and provides excellent results, but one important remaining issue is how the neighbourhood should be chosen. A small neighbourhood of a given vertex as averaging region provides an estimation of the smooth curvature tensor at this vertex, and which is referred to as the ring size [13]. In general, the normal curvature at each vertex can be estimated by the eigenvector of $\mathcal{T}(v)$ associated with the eigenvalue of minimum magnitude. The eigenvalues estimate the principal curvatures k_1 and k_2 at v , also the associated directions are switched: the eigenvector associated with the minimum eigenvalue is the maximum curvature direction, and vice versa for maximum eigenvalue [15].

3. Methodology

The main goal of this work is to produce an accurate system to automatically classify the philtrum that is capable of achieving the results similar to the manual classification produced by an expert [4] and to find the best geometric features for this purpose. Consequently, we evaluate our method on 1000 3D meshes from the ALSPAC data set. The following sections explain in detail the data set, as well as the methods and tools used to achieve this goal.

3.1. Data set

The data of Avon Longitudinal Study of Parents and Children ALSPAC was used in our automatic philtrum classification work; it is a long term health research project involving the study of over 14000 children as they grow up. This study recruited pregnant women living in the former county of Avon in South-West England who had an estimated delivery date of between April 1, 1991 and December 31, 1992. The cohort was made up of 14,541 pregnancies that resulted in 13,971 singletons/twins that were alive at 1 year of age. When the children reached the age of 15 years, their 3D face scans were obtained using two Konica Minolta Vivid 900 laser cameras [16]. After that, twenty one facial landmarks represented by a total of 63 x , y , and z coordinate values were identified and recorded for each 3D facial image by A.M. Toma and A. Zhurov [17]. The landmark points, which can be defined as standard reference points on the faces that have biological meaning, for this data set and their location on the human face are shown in Fig 3.

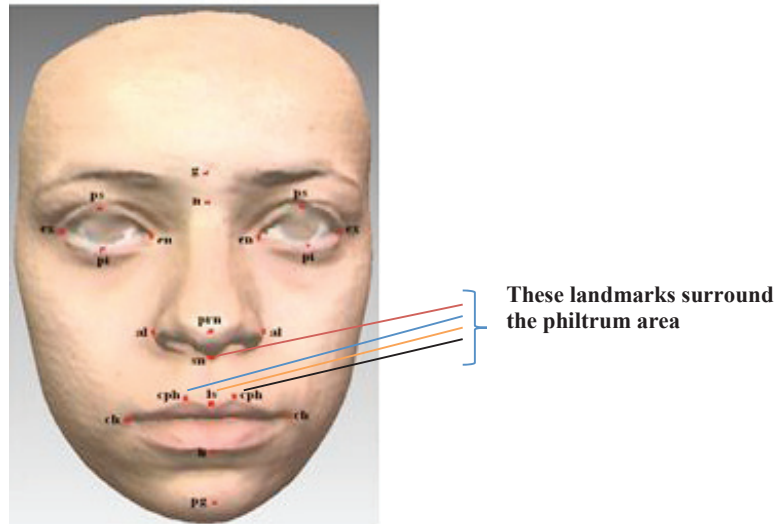


Fig.3 Facial landmarks

3.2. Manual classification

There is a large body of work dedicated to the shape classification of the lips area of the face. In the research carried out by Wilson [4], a large dataset of 4747 3D faces from ALSPAC data set was used. She measured the distances and angles between the landmarks shown in Fig 3 for the lips in general including the philtrum area. From that three categories or classes for the philtrum width are produced (wide, middle, and narrow) which is the same as those used in our automated classification system.

3.3. Feature extraction

The first step of creating any 3D face classification system is building the feature descriptors of the 3D faces. A feature vector is constructed from points distributed over the 3D face as a whole or from certain face region as in our case. In other words, for data set with n 3D faces m feature vectors are produced to construct $n*m$ training and testing matrix. The curvature features are ubiquitous geometric features, easy to extract, the time consumption for processing is very little, and they produced good results in previous research. In this work, the *Maximum*, *Minimum*, *Mean*, *Gaussian*, *Maximum direction*, *Minimum Direction* curvature information was extracted for each face philtrum area and all curvature features were used as a separate entity to form the feature vectors in the training and testing classification set. After that the feature vectors were uniformly quantised to a certain number of bins as described below.

In general, the procedure for extract training and testing sets is:

- Firstly, cutting out the philtrum area of each face according to the landmarks shown in Fig 3.
- Next, calculating the curvature features for the philtrum area using the normal cycle method as described in Section 2.1. Different sizes of the ring (the number of vertices surrounding the vertex that the curvature is calculated for it) were tested in the experimental Section. Algorithm 1 below summarises the process of the computation of curvature features.
- Since the number of features in the curvature features vectors can be different for different philtrums, the vectors are quantised into an equal number of bins using histogram normalization technique [18].
- As a result 36 training and testing sets are obtained, six for each curvature feature.

Algorithm1 curvature features computing

Input: set of vertices V from philtrum area; F mesh faces for philtrum area; R : the ring size.

Output: The maximum and minimum curvature vectors C_{max} , C_{min} ; the maximum and minimum curvature direction matrices U_{min} , U_{max} ; the mean curvature vector C_{mean} ; the Gaussian curvature vector C_{gauss} .
 n is the cardinality of V

For $i=1$ to n **do**

specify the surface area around V_i according to R for which the curvature tensor is estimated

compute the tensor using Eq. 5

calculate the eigenvector u and eigenvalue d of $\mathcal{T}(v)$

$[temp, I]=\text{sort}(d)$

$D(:, i) = d(I)$

$U(:, :, i) = u(:, I)$

end

$U_{min} = U(:, 2, :)$ after removing singleton dimensions from U

$U_{max} = U(:, 1, :)$ after removing singleton dimensions from U

$C_{min} = D(1, :)$

$C_{max} = D(2, :)$

$C_{mean} = (C_{min} + C_{max})/2$

$C_{gauss} = C_{min} \times C_{max}$

3.4. Classification Method

After extracting the feature descriptors from 1000 faces, they were classified using Support Vector Machine (SVM); in particular, LIBSVM was used [19, 20]. For evaluating the performance of our system 5-fold cross-validation method was used.

3.5. Choosing the number of classes

As discussed earlier (Section 3.2), the optimum number of classes manually determined by an expert is *three*. However, we also investigated the optimum number of classes automatically using our chosen curvature features via K-means clustering method [21]. The clustering step is performed after applying Principal Component Analysis to reduce the curvature features dimensionality [22].

4. Implementation and Results

The objectives of our work are classifying the philtrum area width automatically and investigating which curvature features are the best for this purpose, as well as confirming the best number of clusters describing the philtrum area width.

In the previous section it was noted that there is no established method to determine the best ring size for calculating curvature features. Therefore, a range between two and ten vertices was tested for this purpose. After comparing the classification accuracy for each case, the best value was found to be 5 with the classification accuracy reaching 92% when using the *Mean* curvature feature, and 89% and 87% when using the *Max* and *Min* features respectively.

The same process was applied (using the classification results) to determine the best feature descriptor size after they were quantised into 5, 10, 20, 30, 40, and 50 bins. The best classification accuracies were acquired for the descriptor size between 20 and 50 bins. When the descriptor size larger than 50 bins was used the accuracies did not increase dramatically.

Additionally, several features were combined into a single vector to achieve better classification outcomes. The results for feature combinations did not produce better results in all cases. For example when the *Mean* and *Gauss* features were combined, the accuracy of 65% was achieved, while when the *Mean* feature was used alone, the accuracy was 93%, and for *Gauss* feature alone the accuracy was 60%. The best combination of the features was *Max*, *Min*, and *Mean* together, providing classification accuracy of approximately 97%.

The bar chart in Fig. 4 illustrates the classification accuracy for the curvature features as described above. It shows that the features *Mean*, *Max*, and *Min* respectively offered the best classification accuracy result. In contrast, the worst accuracy was achieved by using the *Gauss* curvature and the *Max direction*. Fig. 5 illustrates the dependence of the classification accuracy on the number of bins used in the classification descriptor. Additionally, Fig 5 illustrates the classification accuracy when different features are combined and the system classification accuracy reached 97% when the Mean, Maximum and Minimum curvature features taken together.

Finally, the best number of classes to cluster philtrum features into was investigated from the point of view of the classification accuracy. K-means clustering method was utilized to cluster the compound descriptors of Mean, Min and Max curvature features after applying PCA to reduce the dimensionality of the feature set. The compound features vectors were classified using LIBSVM classifier into two classes with the classification accuracy of 79% and into four classes with the accuracy of 52%. Fig. 6a, b, c and d shows the k-means clustering results for 1000 faces for two, three and four classes. It is clear that the data was separated better using three classes, which corroborates manual expert labelling [4].

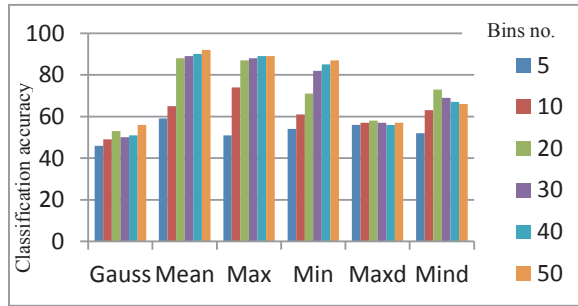


Fig. 4 Classification accuracy for different descriptor sizes

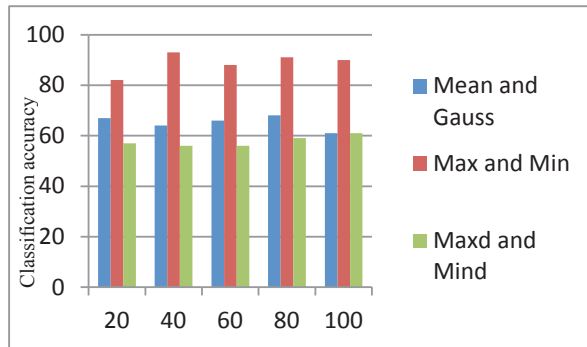


Fig. 5 Classification accuracy for feature combinations

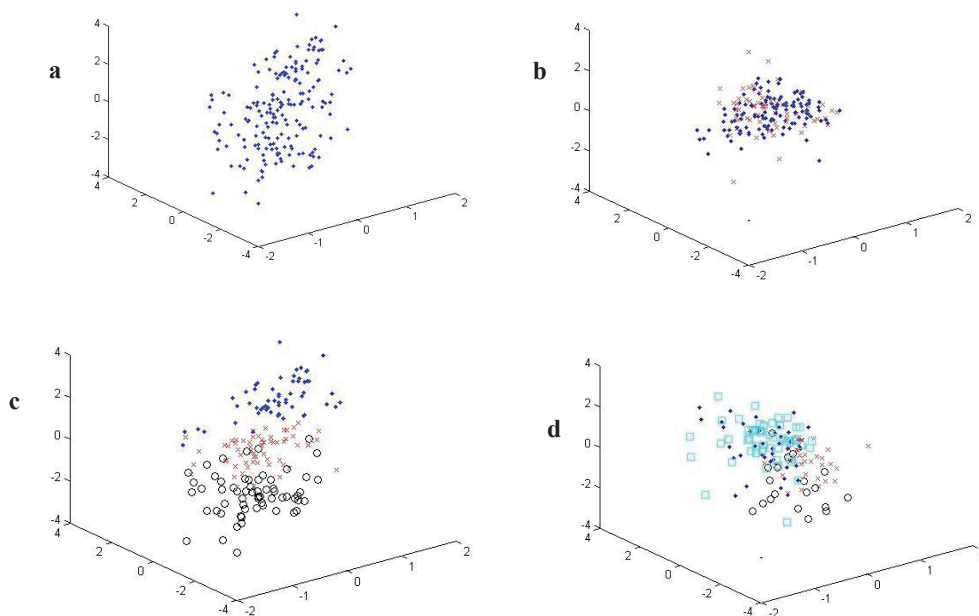


Fig.6 Clustering result (a) the original data (b) $k=2$ (c) $k=3$ (d) $k=4$

5. Conclusion

The goal of our research was to develop a method for automatic classification of facial features for medical applications. In this preliminary study, we focused on creating such a system for philtrum classification, for which we intended to reproduce the classification results obtained manually by Wilson in [4].

In this study, we evaluated the curvature features capability to classify the philtrum face area, found the best curvature feature combination to classify the philtrum into the three classes predetermined by Wilson [4] and investigated the best number of classes of philtrum shapes from the point of view of automatic classification. We compared the automatic classification results to the results produced manually by an expert [4] to assess performance of our system. For the assessment, 1000 3D face meshes were used from ALSPAC dataset with our system achieving 97% classification accuracy in comparison to the ground truth. One of the main challenges in this research was finding the best geometric features to be used in the automatic classification system in order to acquire results close to the manual classification results.

Having developed an automatic method that replicates an expert, we believe we have developed a system with great potential for medical applications (both clinical and research). The analysis of large data sets in whole host is now viable. This could have massive benefit in normative and gene studies where such data sets are essential.

In future, we intend to test the proposed approach in application to other areas of face, such as nose and chin.

Acknowledgements

We are grateful to all researchers and families who took part in establishing the ALSPAC dataset, Dr Caryl Wilson for supplying the necessary information to complete this work and Dr Stephen Richmond for offering valuable advice for this research.

References

- [1] M. Daoudi, A. Srivastava, R. Veltkamp, 3D Face Modeling, Analysis and Recognition, John Wiley & Sons, Ltd,(2013).
- [2] A. Mori, T. Nakajima, T. Kaneko, H. Sakuma, Y. Aoki, Analysis of 109 Japanese children's lip and nose shapes using 3-dimensional digitizer, *British Journal of Plastic Surgery*. 58 (2005) 318–329.
- [3] J.C. Carey, M.M. Cohen, C.J.R. Curry, K. Devriendt, L.B. Holmes, A. Verloes, Elements of morphology: Standard terminology for the lips, mouth, and oral region, *American Journal of Medical Genetics, Part A*. 149 (2009) 77–92.
- [4] C. Wilson, R. Playle, A. Toma, A. Zhurov, A. Ness, S. Richmond, The prevalence of lip vermilion morphological traits in a 15-year-old population, *American Journal of Medical Genetics, Part A*. 161 (2013) 4–12.
- [5] E. Vezzetti, F. Marcolin, 3D human face description: Landmarks measures and geometrical features, *Image and Vision Computing*. 30 (2012) 698–712.
- [6] A.B. Moreno, Á. Sánchez, J.F. Vélez, F.J. Díaz, Face recognition using 3D surface-extracted descriptors, *Irish Machine Vision and Image Processing Conference*, 2003.
- [7] C. Xu, Y. Wang, T. Tan, L. Quan, Automatic 3D face recognition combining global geometric features with local shape variation information, *Automatic Face and Gesture Recognition, FGR, Proceedings of the 6th IEEE International Conference on*. (2004) 308–313.
- [8] S. Ganguly, D. Bhattacharjee, M. Nasipuri, 3D Face Recognition From Range Images Based on Curvature Analysis, *ICTACT Journal on Image*. (2014) 748–753.
- [9] A. Pflug, A. Winterstein, C. Busch, Ear Detection in 3D Profile Images Based on Surface Curvature, *2012 Eighth International Conference on Intelligent Information Hiding and Multimedia Signal Processing*. (2012) 1–6.

- [10] L. Chen, S. Biswas, Digital Curvatures Applied to 3D Object Analysis and Recognition: case study, Springer, Lecture Notes in Computer Science. (2009).
- [11] Y. Wang, M. Meng, Q. Zhen, Learning encoded facial curvature information for 3D facial emotion recognition, Proceedings - 2013 7th International Conference on Image and Graphics, ICIIG (2013) 529–532.
- [12] S. Petitjean, A survey of methods for recovering quadrics in triangle meshes, ACM Computing Surveys. 34 (2002) 211–262.
- [13] D. Cohen-Steiner, J.-M. Morvan, Restricted delaunay triangulations and normal cycle, Proceedings of the Nineteenth Conference on Computational Geometry. (2003) 312-321.
- [14] J.-M.M. Xing Sun, Curvature measures, normal cycles and asymptotic cones, Actes Des Rencontres Du C.I.R.M. 3 (2013) 3–10.
- [15] P. Alliez, D. Cohen-Steiner, O. Devillers, B. Lévy, M. Desbrun, Anisotropic polygonal remeshing, ACM Transactions on Graphics. 22 (2003) 485.
- [16] C.H. Kau, S. Richmond, Three-dimensional analysis of facial morphology surface changes in untreated children from 12 to 14 years of age, American Journal of Orthodontics and Dentofacial Orthopedics. 134 (2008) 751–760.
- [17] M. Toma, A. Zhurov, R. Playle, E. Ong, S. Richmond, Reproducibility of facial soft tissue landmarks on 3D laser-scanned facial images, Orthodontics and Craniofacial Research. 12 (2009) 33–42.
- [18] L. Mioulet, T.P. Breckon, A. Mouton, H. Liang, T. Morie, Gabor features for real-time road environment classification, Proceedings of the IEEE International Conference on Industrial Technology. (2013) 1117–1121.
- [19] Chih-Wei Hsu, Chih-Chung Chang, A Practical Guide to Support Vector Classification. (2010).
- [20] David Meyer, Support Vector Machines, FH Technikum Wien, Austria (2014).
- [21] T. Kanungo, D.M. Mount, N.S. Netanyahu, C.D. Piatko, R. Silverman, A.Y. Wu, An efficient k-means clustering algorithm: analysis and implementation, IEEE Transactions on Pattern Analysis and Machine Intelligence. 24 (2002) 881–892.
- [22] L.I. Smith, A tutorial on Principal Components Analysis, Cornell University, USA. (2002).